

1-1-2012

Conformal Cosmology and the Pioneer Anomaly

Gabriele U. Variieschi

Loyola Marymount University, gvarieschi@lmu.edu

Repository Citation

Variieschi, Gabriele U., "Conformal Cosmology and the Pioneer Anomaly" (2012). *Physics Faculty Works*. 9.
http://digitalcommons.lmu.edu/phys_fac/9

Recommended Citation

G. Variieschi, "**Conformal cosmology and the Pioneer Anomaly**," *Phys. Res. Int.* 2012:469095, 2012.

This Article is brought to you for free and open access by the Seaver College of Science and Engineering at Digital Commons @ Loyola Marymount University and Loyola Law School. It has been accepted for inclusion in Physics Faculty Works by an authorized administrator of Digital Commons@ Loyola Marymount University and Loyola Law School. For more information, please contact digitalcommons@lmu.edu.

Research Article

Conformal Cosmology and the Pioneer Anomaly

Gabriele U. Varieschi

Department of Physics, Loyola Marymount University, Los Angeles, CA 90045, USA

Correspondence should be addressed to Gabriele U. Varieschi, gvarieschi@lmu.edu

Received 9 August 2011; Revised 9 October 2011; Accepted 10 October 2011

Academic Editor: A. Beesham

Copyright © 2012 Gabriele U. Varieschi. This is an open access article distributed under the Creative Commons Attribution License, which permits unrestricted use, distribution, and reproduction in any medium, provided the original work is properly cited.

We review the fundamental results of a new cosmological model, based on conformal gravity, and apply them to the analysis of the early data of the Pioneer anomaly. We show that our conformal cosmology can naturally explain the anomalous acceleration of the Pioneer 10 and 11 spacecrafts, in terms of a local blueshift region extending around the solar system and therefore affecting the frequencies of the navigational radio signals exchanged between Earth and the spacecraft. By using our model, we explain the numerical coincidence between the value of the anomalous acceleration and the Hubble constant at the present epoch and also confirm our previous determination of the cosmological parameters $\gamma \sim 10^{-28} \text{ cm}^{-1}$ and $\delta \sim 10^{-4}-10^{-5}$. New Pioneer data are expected to be publicly available in the near future, which might enable more precise evaluations of these parameters.

1. Introduction

The Pioneer 10 and 11 spacecrafts were launched in the early 1970s, to conduct explorations in the region of the solar system beyond the orbit of Mars and to perform close observations of Jupiter. They were also the first spacecraft to explore the outer solar system and to send back to Earth their navigational signals for almost thirty years (for a review see [1] and references therein).

In recent years, the orbits of Pioneer 10 and 11 were reconstructed very accurately, by using the original radiometric Doppler tracking data, based on the signals exchanged between the spacecraft and NASA's terrestrial tracking stations. This reconstruction yielded a persistent discrepancy between the observed and predicted data, equivalent to an unexplained small acceleration of the spacecraft in the direction of the Sun. This effect is evidenced by measuring a small frequency shift (toward higher frequencies, i.e., a "blueshift") of the signal reaching us from the spacecraft. The nature of this anomalous acceleration or of the related blueshift remains unexplained; this effect has become known as the "Pioneer anomaly" ([2–4]).

This is not the only known gravitational anomaly in the solar system, since several others are currently under investigation (for general reviews see [5, 6]), such as the secular

increase of the astronomical unit [7], the anomalies in planetary flybys ([8–10]), the anomalous perihelion precession of Saturn ([11, 12]), the increase in the eccentricity of the Moon's orbit ([13, 14]), and other effects related in general with ephemerides of planets and the Moon ([15, 16]).

The importance of all these effects is not related to how they affect the spacecraft navigation, since they all produce very small corrections to the orbits, but to the possibility that these anomalies might be an indication of new gravitational physics. In particular, several nonconventional explanations of these effects have been proposed (see general discussion in [1, 2, 4]) such as modifications of the law of gravity, or a modified inertia, as proposed by the Modified Newtonian Dynamics (MOND) theory, the existence of a dark matter halo around the Earth, or in the solar system, which might slightly alter the gravitational force acting on the spacecraft, and several others ([17–21]).

In this line of reasoning, alternative gravitational theories such as conformal gravity (CG), originally proposed by Weyl in 1918 ([22–24]) and revisited by Mannheim and Kazanas ([25–27]), have provided a new framework for cosmological models, with the advantage of avoiding some of the most controversial elements of current standard cosmology, such as dark matter, dark energy, inflation, and others.

Following the original CG, we have recently studied an alternative approach to these models which was named “kinematical conformal cosmology” [28], but that for brevity will be called conformal cosmology (CC) in the rest of this paper. This approach was based on the direct application of the conformal symmetry to the Universe, that is, considering the possibility that a “stretching” of the spacetime fabric might be acting over cosmological scales. In a second part of this work [29], it was shown that this model can successfully fit type-Ia Supernovae data, without assuming the existence of dark matter or dark energy.

A preliminary analysis also performed in our second paper [29] indicated that CC might be able to explain the existence of the Pioneer anomaly, since the observed blueshift of the spacecraft signal could be due to a region of cosmological blueshift surrounding our solar system, which is naturally predicted by our model. A new comprehensive review of the Pioneer anomaly has been published [1], together with more details of the Pioneer early data [30], thus prompting us to reconsider and improve our previous analysis [29], based on the conformal cosmology approach. In addition, a revised analysis of the Pioneer anomaly, based on extended data sets, has recently appeared in the literature [31], confirming the existence of the anomaly and adding new insights into its temporally varying behavior.

In the next section, we will briefly review our CC solutions, showing how a local blueshift region can naturally emerge, while, in Section 3, we will fit all current Pioneer data [30] with our cosmological solutions and determine the values of the parameters in our model. Finally, in Section 4, we will discuss our results and compare them to the existing physical limits of standard gravity in the solar system.

2. Conformal Cosmology

In our first CC paper [28], we used as a starting point the line element originally derived by Mannheim and Kazanas [25] as an exterior solution for a static, spherically symmetric source in conformal gravity theory, that is, the analogue of the Schwarzschild exterior solution in general relativity:

$$ds^2 = -B(r)c^2 dt^2 + \frac{dr^2}{B(r)} + r^2 d\psi^2, \quad (1)$$

where $d\psi^2 = d\theta^2 + \sin^2\theta d\phi^2$ in spherical coordinates and

$$B(r) = 1 - \frac{\beta(2 - 3\beta\gamma)}{r} - 3\beta\gamma + \gamma r - \kappa r^2, \quad (2)$$

with the parameters $\beta = MG/c^2$ (cm), γ (cm^{-1}), κ (cm^{-2}), where M is the mass of the (spherically symmetric) source and G is the gravitational constant. Conformal gravity introduces two new parameters γ and κ which are not present in standard general relativity, while the familiar Schwarzschild solution is recovered in the limit for $\gamma, \kappa \rightarrow 0$, in the equations above.

We then considered regions far away from matter distributions, thus ignoring the matter dependent β terms, and rewrote the last equation in a simplified form:

$$B(r) = 1 + \gamma r - \kappa r^2 = 1 + \gamma r + \left(\frac{\gamma^2}{4} + k\right)r^2 = -g_{00}(r), \quad (3)$$

where the parameter k is linked to γ and κ , through $k = -\gamma^2/4 - \kappa$, and it is ultimately connected to the so-called trichotomy constant \mathbf{k} (in bold) of a Robertson-Walker (RW) metric, defined as $\mathbf{k} \equiv k/|k| = 0, \pm 1$. This is also related to another fundamental aspect of CG: the existence of coordinate and conformal transformations connecting the static, spherically symmetric solution represented by (1) and (3), with the classical Robertson-Walker metric (see details in [28]).

It was precisely this connection between the two solutions which prompted us to consider the CG static, spherically symmetric solution as an alternative description of the standard cosmological evolution, based on the RW metric. In other words, the CG static solution might also contain information about the cosmological redshift, the expansion of the Universe, and so forth, and constitute an alternative approach to cosmology. In particular, the CG expressions in (2) or (3) contain a linear and a quadratic term, in the radial coordinate r , which might yield considerable effects at large distances, (by using the contribution of the linear term γr , the flat galactic rotation curves were in fact explained by Mannheim ([32, 33]) without the need of dark matter.) including a strong gravitational redshift which could be, at least in part, responsible for the observed cosmological redshift.

Therefore, we postulated in [28] that the observed redshift is due to this gravitational effect, which influences the wavelength or frequency of a light signal emitted at time t and position r , and observed at the origin ($r = 0$) at the current time t_0 , in the following way:

$$1 + z = \frac{R(0)}{R(r)} = \frac{\lambda(r, t)}{\lambda(0, t_0)} = \frac{\nu(0, t_0)}{\nu(r, t)} = \sqrt{\frac{-g_{00}(0)}{-g_{00}(r)}} \quad (4)$$

$$= \frac{1}{\sqrt{1 + \gamma r + (\gamma^2/4 + k)r^2}}.$$

In the previous equation, the redshift factor $(1 + z)$ is related to the ratio of cosmic scale factors R , which simply depend on the radial distance r , in view of (3). Alternatively, to obtain a time-dependent form of the cosmic scale factor, we considered that the radial distance r is associated with a look-back time $(t_0 - t)$, related to the time of travel of a light signal. Integrating the CG metric in (1) and (3) along the null geodesic, we obtained [28]

$$1 + z = \frac{R(t_0)}{R(t)} = \left(\cos \chi - \delta \sin \chi\right), \quad k > 0,$$

$$1 + z = \frac{R(t_0)}{R(t)} = \left(1 - \delta \chi\right), \quad k = 0, \quad (5)$$

$$1 + z = \frac{R(t_0)}{R(t)} = \left(\cosh \chi - \delta \sinh \chi\right), \quad k < 0,$$

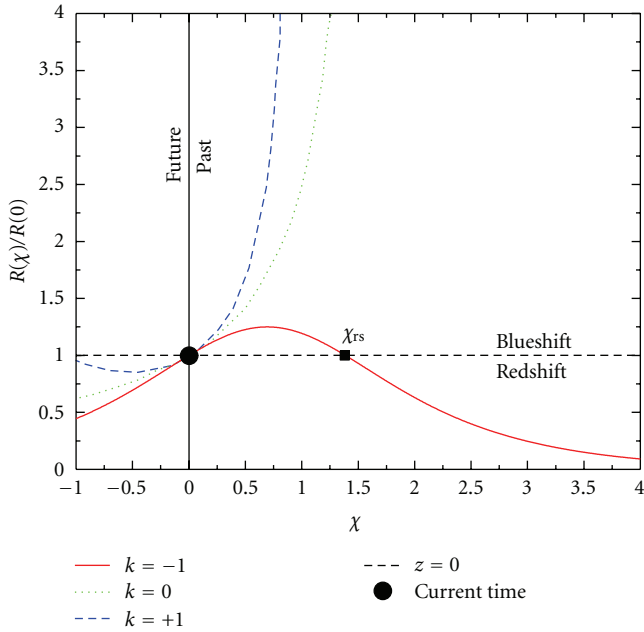


FIGURE 1: R functions obtained from (5) are shown here for different values of \mathbf{k} : $\mathbf{k} = -1$ in red (solid), $\mathbf{k} = 0$ in green (dotted), and $\mathbf{k} = +1$ in blue (dashed), and, for a positive value of the parameter $\delta \cong 0.6$ (an unrealistically large value, our current value $\delta = \delta(t_0)$ will be shown to be positive and close to zero).

for the three possible values of the parameter k . In the previous equation, we preferred to use dimensionless quantities and parameters, defined as follows:

$$\chi \equiv \sqrt{|k|}c(t_0 - t), \quad \delta \equiv \frac{\gamma}{2\sqrt{|k|}}, \quad (6)$$

so that the fundamental parameters of our conformal cosmology are now expressed by $\gamma(\text{cm}^{-1})$ and the dimensionless δ (c is the speed of light in vacuum, assumed constant).

In Figure 1, we plot the results of (5) in terms of the inverse ratio $R(\chi)/R(0) = R(t)/R(t_0) = 1/(1+z)$ which describes better the cosmic evolution. The dimensionless quantity $\chi \equiv \sqrt{|k|}c(t_0 - t)$, on the horizontal axis, represents a look-back time, so that the universal evolution of the cosmic scale factor, from the past to the future, can be seen by following our curves from right to left. The circular dot on the vertical axis represents our “current time” ($\chi = 0$). We can clearly see that the only solution which shows a redshift in the past (values below the horizontal black dashed line, representing $z = 0$) is the red-solid curve, corresponding to $\mathbf{k} = -1$. Therefore, the other two solutions, for $\mathbf{k} = +1, 0$, are ruled out; only the $\mathbf{k} = -1$ solution will be considered in the following.

Our preferred solution in Figure 1 (red-solid) also shows a blueshift region in the immediate past of our current time, which in Section 3 will be related directly to the Pioneer anomaly. This blueshift region is greatly exaggerated in the figure, since the different curves were plotted for $\delta \simeq 0.6$, an unrealistically high value. We will show in the next sections that δ is positive and close to zero, resulting in a

very small-sized blueshift region, compared to the overall size of the Universe. Similar plots can be obtained for the ratio R/R_0 expressed in terms of the radial distance r (see [28] for details), which also suggest the existence of a blueshift region localized around the observer’s position, that is, the Earth could be surrounded by a natural blueshift region, extending at least over the solar system region. This might be the origin of the Pioneer anomaly. (Obviously, the Earth’s observer is not located at any privileged position. The same cosmological evolution described by CC would be seen by any other observer in the Universe, provided that the local values of the cosmological parameters δ and γ are the same. In our previous work ([28, 29]), we have suggested that δ might play the role of a universal time, so that for a certain value of this parameter the evolution of the Universe would look the same for any observer. In this way, conformal cosmology does not violate the cosmological principle, which postulates a homogeneous and isotropic Universe.)

Before we proceed to analyze this possible explanation for the anomaly, we recall a few more results obtained in our second paper [29]. Since we have closed-form expressions for our scale factor R , in (4) and (5), it is straightforward to obtain the Hubble parameter ($H(t) = \dot{R}(t)/R(t)$) and the deceleration parameter ($q(t) = -\ddot{R}(t)/R(t)H^2(t) = -\ddot{R}(t)R(t)/\dot{R}^2(t)$) as a function of time or redshift z . For the $\mathbf{k} = -1$ case, we obtained [29]

$$\begin{aligned} H(t) &= \sqrt{|k|}c \left(\frac{\sinh \chi - \delta \cosh \chi}{\cosh \chi - \delta \sinh \chi} \right) \\ &= \pm \sqrt{|k|}c \frac{\sqrt{(1+z)^2 - (1-\delta^2)}}{(1+z)}, \end{aligned} \quad (7)$$

$$\begin{aligned} q(t) &= \left(\frac{\cosh \chi - \delta \sinh \chi}{\sinh \chi - \delta \cosh \chi} \right)^2 - 2 \\ &= \frac{(1+z)^2}{(1+z)^2 - (1-\delta^2)} - 2, \end{aligned}$$

and, in particular for $\chi \rightarrow 0$ or $z \rightarrow 0$,

$$\begin{aligned} H(t_0) &= -\frac{\gamma}{2}c, \quad H(z=0) = \pm \frac{\gamma}{2}, \\ q(t_0) &= q(z=0) = \frac{1}{\delta^2} - 2. \end{aligned} \quad (8)$$

The signs of the quantities in (7) and (8) can be explained by considering again the red-solid curve in Figure 1, which represents the ratio $R(\chi)/R(0)$, or equivalently $R(t)/R(t_0)$, over different cosmological epochs. This bell-shaped curve was plotted for a positive value of δ and shows a local blueshift area in the “past” evolution of the Universe, extending back to $\chi_{rs} = \text{arccosh}[(1+\delta^2)/(1-\delta^2)] = 2 \text{ arctanh } \delta$ (represented by the square point in Figure 1) or $(t_0 - t_{rs}) = (2/\sqrt{|k|}c) \text{ arctanh } \delta$, for the look-back time at which the redshift (rs) starts being observed. The red

curve has a maximum at $\chi_{\max} = \operatorname{arctanh} \delta$ or $(t_0 - t)_{\max} = (1/\sqrt{|k|} c) \operatorname{arctanh} \delta$ (we can also find $(R(\chi)/R(0))_{\max} = 1/\sqrt{1 - \delta^2}$ or $z_{\min} = \sqrt{1 - \delta^2} - 1$), and it is evidently symmetric around this point of maximum expansion of the Universe.

Therefore, for each value of z , that is, for each value of $R(\chi)/R(0)$, we have two corresponding values of the Hubble parameter (except at the maximum, for $z_{\min} = \sqrt{1 - \delta^2} - 1$, where $H = 0$). The two related points on the curve, at the same redshift level, will have equal and opposite expansion rates. This yields the double sign in the previous expressions for H , when given as a function of z . This argument applies also to the $z = 0$ case, corresponding to the current time t_0 , at which $H(t_0) = -(\gamma/2)c$ is negative, showing that the Universe is already in a contracting phase. (This is also a consequence of the signs of our conformal parameters, in particular the positive value of γ . Our estimate of γ will be given in Section 3, but we recall that Mannheim has independently evaluated γ as a small but positive quantity ($\gamma_{\text{Mann}} = 3.06 \times 10^{-30} \text{ cm}^{-1}$), by fitting rotational velocity curves for several spiral galaxies, using conformal gravity [27]. If γ was to have a negative value, we would still be in an expanding phase of the Universe.) As discussed above, the same $z = 0$ value can also refer to the time in the past (t_{rs}) at which we start observing the cosmological redshift, with $H(t_{\text{rs}}) = +(\gamma/2)c$, a positive quantity. This analysis does not contradict the current astrophysical estimates of H_0 as a positive quantity. They are based on redshift observations of light coming from galaxies at times in the past $t \lesssim t_{\text{rs}}$; therefore, what is denoted by H_0 in standard cosmology should be actually indicated as $H(t_{\text{rs}}) = +(\gamma/2)c$, again a positive quantity related to the expanding phase of the Universe. The same analysis can be done in terms of radial distances r . The blueshift region would extend from $r = 0$ up to a distance given by

$$r_{\text{rs}} = \frac{\gamma}{|k| - \gamma^2/4} = \frac{4}{\gamma} \frac{\delta^2}{1 - \delta^2}, \quad (9)$$

where r_{rs} is the distance at which we start observing the cosmological redshift. In general, the slope of the red-solid curve in Figure 1 is related to the value of the Hubble parameter at that point, while its curvature is connected to the deceleration parameter, through the expressions given above.

In particular, following (8), the slope of the plot and its curvature at current time t_0 are basically connected to our two fundamental parameters γ and δ . In the next section, we will show that the slope of the red-solid plot at t_0 is closely related to the value of the Pioneer anomalous acceleration a_P , which can therefore be used to determine γ . Similarly, the curvature of the plot at t_0 will be related to the rate of change of the anomalous acceleration (i.e., the ‘‘jerk’’ $j_P \equiv \dot{a}_P$) and will be used to determine the value of our other parameter δ .

We conclude this section by noting that the values of our parameters (δ and γ) could be derived directly from standard cosmological observations, in view of (8). Using the current best estimate of $H_0 = (72 \pm 3) \text{ km s}^{-1} \text{ Mpc}^{-1}$ [34] and the positive sign in (8), we obtain

$$\gamma = \frac{2H_0}{c} = (1.56 \pm 0.06) \times 10^{-28} \text{ cm}^{-1}. \quad (10)$$

The direct determination of δ is more difficult, since the deceleration parameter q is not known explicitly. In [29], we based our analysis on recent luminosity data for type-Ia Supernovae, obtaining an estimate of $\delta \simeq 3.83 \times 10^{-5}$, but this analysis needs to be confirmed by further studies.

3. The Pioneer Anomaly

In the previous section, we briefly reviewed our conformal cosmology and outlined the reasons why we consider the $\mathbf{k} = -1$ solution as a possible description of the evolution of the Universe. This solution can explain the observed cosmological redshift, but it requires the existence of a blueshift region in the immediate vicinity of our current spacetime position in the Universe.

This could be a serious problem for our model, since we do not observe blueshift of nearby astrophysical objects except for the one caused by the peculiar velocities of nearby galaxies, presumably due to standard Doppler shift. However, as already mentioned in Section 1, experimental evidence of a local region of blueshift might come from the analysis of the Pioneer anomaly ([1–4, 30, 35–42]).

This is a small frequency drift (blueshift), observed analyzing the navigational data of the Pioneer 10–11 spacecraft, received from distances between 20 and 70 AU (astronomical units) from the Sun, while these spacecraft were exploring the outer solar system. This anomaly is usually reported as a positive rate of change of the signal frequency, $\dot{\nu}_P > 0$ (blueshift), resulting in a frequency drift of about 1.5 Hz every 8 years, or as an almost constant sunward acceleration, $a_P < 0$, or even as a ‘‘clock acceleration’’ $a_t \equiv a_P/c < 0$. More precisely ([1, 35]),

$$\begin{aligned} \dot{\nu}_P &= (5.99 \pm 0.01) \times 10^{-9} \text{ s}^{-2}, \\ a_P &= -(8.74 \pm 1.33) \times 10^{-8} \text{ cm s}^{-2}, \\ a_t \equiv \frac{a_P}{c} &= -(2.92 \pm 0.44) \times 10^{-18} \text{ s}^{-1}. \end{aligned} \quad (11)$$

An attempt was made to detect such anomaly also in the radiometric data from other spacecraft traveling at the outskirts of the solar system, such as the Galileo and Ulysses missions [35]. In the case of Galileo, the effects of solar radiation made such detection impossible, while for Ulysses a possible anomalous acceleration $a_{\text{Ulysses}} = -(12 \pm 3) \times 10^{-8} \text{ cm/s}^2$ was seen in the data. Other spacecraft, such as the New Horizons mission to Pluto, launched in 2006, might provide new data in the near future. These discoveries prompted a complete reanalysis of all the historical navigational data of these space missions, which is currently underway ([1, 31, 37–39, 42, 43]) and will be completed in the near future [44]. This new analysis will try to determine additional characteristics of the anomaly, such as its precise direction, the possible temporal and spatial variations, and its dependence on heliocentric or geocentric distance. A future dedicated mission is also being proposed ([45–48]) to test directly this puzzling phenomenon.

Currently, the origin and nature of this anomaly remains unexplained; all possible sources of systematic errors have

been considered ([1, 4, 35, 36, 39, 43, 49]), but they cannot fully account for the observed effect. The current focus of conventional explanations of the anomaly seems to be the thermal recoil force, that is, anisotropically emitted thermal radiation, originating from the spacecraft four radioisotope thermoelectric generators (RTGs), which can contribute significantly to the measured acceleration. The natural decay of the radioactive material in the RTGs, the aging of the thermocouples in the system, and other effects all contribute to the decrease of the total thermal power during the spacecraft life. This might explain the decrease overtime of the measured Pioneer acceleration (in absolute value), that is, the negative “jerk” $d|a_P|/dt < 0$, already seen in the early Pioneer data ([1, 30, 44]).

Several other papers ([50–56]) recently appeared in the literature, dealing with plausible explanations of the Pioneer Anomaly, in terms of mundane, nongravitational forces.

Although the anomaly can be caused by these standard physical effects, we will try in the following to explain its origin by using the cosmological model outlined in the previous section. The phenomenology of the Pioneer anomaly is related to a complex exchange of radiometric signals between the tracking stations on Earth (of the deep space network (DSN)) and the spacecraft, using S-band Doppler frequencies (1.55–5.20 GHz). Typically, an uplink signal is sent from the DSN to the spacecraft at a frequency of 2.11 GHz, based on a very stable hydrogen maser system, then an S-band transponder on board the spacecraft applies an exact and fixed turn-around ratio of 240/221 to the uplink signal, so that the Pioneer returns a downlink signal at a slightly different frequency of about 2.29 GHz, to avoid interference with the uplink one.

This procedure is known as a two-way Doppler coherent mode and allows for very precise tracking of the spacecraft, since the returning signal is directly compared to the original one. On the contrary, a one-way Doppler signal (with a fixed signal source on the spacecraft, whose frequency cannot be monitored for accuracy) is less effective. This type of tracking system added to the propulsion and navigational characteristics of the Pioneer spaceship (especially the presence of a spin-stabilization system) resulted in a very good acceleration sensitivity of about 10^{-8} cm/s², once the influence of solar radiation pressure can be neglected (for distances $\gtrsim 20$ AU from the Sun).

The DSN station acquires the downlink signal after a time delay ranging from a few minutes to some hours, depending on the distance involved, and compares it to the reference frequency to determine the Doppler shift due to the actual motion of the spacecraft. The navigational software can also model with great precision the expected frequency of the signal returned from the Pioneer, which should coincide with the one observed on Earth. As already mentioned, a discrepancy was found, corresponding to the values in (11), whose origin cannot be traced to any systematic effect due to either the performance of the spacecraft or the theoretical modeling of its navigation.

The Pioneer anomaly was first reported ([2–4]) as an almost constant value of the anomalous acceleration, with temporal and space variation of a_P within 10%, over a range

of heliocentric distances ~ 20 –70 AU, and possibly at even closer distances $\lesssim 10$ AU, so that we will concentrate first on the average value of a_P and later on its variation with time and distance. In our view, the Pioneer phenomenology represents the most basic experiment we could perform in order to check if the cosmic evolution is really affecting the frequency of electromagnetic radiation emitted and observed at different spacetime locations, following (4) and (5).

In the standard analysis of the Pioneer anomaly, the signal coming back to Earth is affected by the relativistic Doppler effect. Following this model, ν_{mod} will be the frequency of the expected signal and will be related to the signal reference frequency $\nu_{\text{ref}} = 2.11$ GHz (for the uplink signal in a two-way system) by the standard relativistic Doppler formula (see equation 2.2.2 in [57]):

$$\frac{\nu_{\text{mod}}}{\nu_{\text{ref}}} = \frac{\sqrt{1 - \mathbf{v}^2/c^2}}{1 + \nu_r/c} \simeq 1 - \frac{\nu_r}{c}, \quad (12)$$

where ν_r is the spacecraft radial velocity and the approximation on the right-hand side holds to first order in ν_r/c .

Since we have a two-way system, the Doppler shift involved is actually double, so we can use the previous equation but with $\nu_r = 2\nu_{\text{mod}}(t')$, where $\nu_{\text{mod}}(t')$ is the expected velocity of the spacecraft, according to the theoretical navigation model, at time t' , when the spaceship receives and immediately retransmits the signal. We use here a time variable t' which can be simply considered the elapsed time since the spacecraft launch ($t' = 0$ at $r = 0$), and then later we will simply identify t' with our cosmological look-back time ($t_0 - t$) in (6). With this radial velocity, (12) to first order in ν_r/c becomes

$$\nu_{\text{mod}}(t') \simeq \nu_{\text{ref}} \left[1 - \frac{2\nu_{\text{mod}}(t')}{c} \right], \quad (13)$$

and this frequency is expected to be observed with high precision, due to the reported excellent navigational control of the spacecraft.

On the contrary, a different frequency is observed, $\nu_{\text{obs}}(t') > \nu_{\text{mod}}(t')$, involving an additional unexplained blueshift: this is the Pioneer anomaly. Following (11), the frequency difference is reported as

$$\begin{aligned} \Delta\nu(t') &= \nu_{\text{obs}}(t') - \nu_{\text{mod}}(t') \simeq 2t' \dot{\nu}_P, \\ \dot{\nu}_P &= 5.99 \times 10^{-9} \text{ s}^{-2} \quad (\text{one-way}), \end{aligned} \quad (14)$$

where the factor of two in the first line of the previous equation is due to the two-way system. We also remark here that several of the cited references adopt a rather confusing “DSN sign convention” for the frequency difference in (14) (see [1, 4, 38] and (38) of [2]), resulting in a change of sign in most of their equations. We prefer to use here our definition of $\Delta\nu$ as given in the previous equation.

The anomalous acceleration a_P is introduced as an alternative way of describing the effect, although, in our view, it does not correspond to a real spacecraft acceleration. As in (13), we can write the observed frequency to first order in ν_r/c as

$$\nu_{\text{obs}}(t') \simeq \nu_{\text{ref}} \left[1 - \frac{2\nu_{\text{obs}}(t')}{c} \right], \quad (15)$$

where the “observed” velocity of the spacecraft refers to the time of interest t' . Combining together the last three equations, we can write the frequency difference as

$$\Delta\nu(t') = -2\frac{\nu_{\text{ref}}}{c}[\nu_{\text{obs}}(t') - \nu_{\text{mod}}(t')] = -2\frac{\nu_{\text{ref}}}{c}\Delta\nu(t'). \quad (16)$$

These frequency differences $\Delta\nu$ (also called frequency residuals in the literature cited) are therefore equivalent to the corresponding velocity residuals ($\Delta\nu = \nu_{\text{obs}} - \nu_{\text{mod}}$), and they are usually plotted as a function of the elapsed time t' , showing an almost linear increase with time of these residuals, which is the essence of the Pioneer anomaly (see, e.g., Figure 5.2 in [1]). The Pioneer anomalous acceleration can be defined as the rate of change of the velocity residuals, related to the corresponding rate of change of the frequency residuals, in view of (16). Therefore, if we define $a_P \equiv d(\Delta\nu)/dt'$, the Pioneer acceleration can be related to the frequency differences

$$a_P = \frac{d(\Delta\nu)}{dt'} = -\frac{c}{2\nu_{\text{ref}}}\frac{d(\Delta\nu)}{dt'}, \quad (17)$$

which are more significant quantities in our analysis. We will assume that these frequency differences are intrinsically due to the different locations of the spacecraft (at position r) and of the Earth’s observer (at $r = 0$). Therefore, we identify the reference frequency ν_{ref} in (13) with $\nu(0)$ and the similar quantity ν_{ref} in (15) with $\nu(r)$. Then, we subtract (13) from (15):

$$\begin{aligned} \Delta\nu(t') &= 2[\nu(r) - \nu(0)]\left[1 - \frac{2\nu(t')}{c}\right] \simeq 2[\nu(r) - \nu(0)] \\ &= 2\nu(0)\left[\frac{\nu(r)}{\nu(0)} - 1\right] = 2\nu_{\text{ref}}\left[\frac{R(r)}{R(0)} - 1\right] \\ &= 2\nu_{\text{ref}}\left[\frac{R(t')}{R(0)} - 1\right] \simeq 2\nu_{\text{ref}}\left[\frac{\gamma}{2}ct'\right], \end{aligned} \quad (18)$$

where the common factor of two in all the parts of the previous equation was added again because of the two-way effect, which has to be included also in our gravitational blueshift model. The velocities $\nu_{\text{mod}}(t')$ and $\nu_{\text{obs}}(t')$ from (13) and (15) are assumed to be the same, so that the common factor $[1 - 2\nu(t')/c] \simeq 1$ is close to unity and can be neglected, since the average Pioneer speed is $\nu_P \simeq 12.8 \text{ km/s} \ll c$ [58]. We also identified $\nu(0)$ with the Earth reference frequency ν_{ref} and used our fundamental equation (4) and (5), $k < 0$ case, to first order in $\chi = \sqrt{|k|}ct'$. (The elapsed time t' for the Pioneer spacecraft missions is of the order of a few years ($1 \text{ yr} = 3.156 \times 10^7 \text{ s}$); we can assume $\sqrt{|k|} \sim \gamma \sim 10^{-28}\text{--}10^{-30} \text{ cm}^{-1}$; therefore, $\sqrt{|k|}ct' \sim 10^{-10}\text{--}10^{-12} \ll 1$.) Using these results, (17) simplifies as follows:

$$a_P = a_P(t_0) = -\frac{\gamma}{2}c^2 = cH(t_0), \quad (19)$$

in view also of our evaluation of $H(t_0) = -(\gamma/2)c$ (a negative quantity) from (8).

This result immediately explains the often cited “numerical coincidence,” that is, the simple relation $|a_P| \simeq cH_0$

between the Pioneer acceleration and the standard (positive) Hubble constant, with the correct negative sign for both quantities in (19), in view of our previous discussion of the sign of $H(t_0) < 0$. Equation (19) can also be used to determine γ and H_0 (as a positive quantity), using the reported value of a_P from (11):

$$\begin{aligned} \gamma &= \gamma(t_0) = -\frac{2}{c^2}a_P = (1.94 \pm 0.30) \times 10^{-28} \text{ cm}^{-1}, \\ H_0 &= (90.0 \pm 13.7) \text{ km s}^{-1} \text{ Mpc}^{-1}. \end{aligned} \quad (20)$$

The value of γ (considered measured at the current time t_0 , even if the Pioneer data are a few years old) is close to our first direct estimate in (10), and the corresponding value of the Hubble constant is close to the value of standard cosmology. We remark here again that our model fully explains the reason of this “numerical coincidence” and provides also the correct signs for all the quantities involved. (The numerical “coincidence” between the Hubble constant and the value of the Pioneer acceleration a_P divided by c was noticed immediately after the discovery of the Pioneer effect and prompted many speculations and different explanations. This coincidence is even more striking if one uses the value cited in [4] as the experimental value for Pioneer 10 data before systematics, $a_P = -7.84 \times 10^{-8} \text{ cm s}^{-2}$, thus obtaining $H_0 = 80.7 \text{ km s}^{-1} \text{ Mpc}^{-1}$ and $\gamma_0 = 1.74 \times 10^{-28} \text{ cm}^{-1}$.)

Following (17)–(19) and the related discussion, we can generalize our expression of the Pioneer acceleration, as a function of time t' :

$$a_P = -c\frac{d[R(t')/R(0)]}{dt'} = c^2\frac{\gamma}{2\delta}\left[\frac{\sinh \chi - \delta \cosh \chi}{\cosh \chi - \delta \sinh \chi}\right]^2, \quad (21)$$

with $\chi = \sqrt{|k|}ct' = (\gamma/2\delta)ct'$. (Although t' is the elapsed time since the spacecraft launch, it is treated here as equivalent to a look-back time ($t_0 - t$) because the Pioneer is moving toward increasing distances r , therefore corresponding to increased look-back times in our original redshift interpretation.) In particular, by using the previous equation and taking another time derivative, it is easy to derive the “jerk” $j_P \equiv da_P/dt'$ and its value in the limit for $t' \rightarrow 0$:

$$j_P = j_P(t_0) = c^3\left(\frac{\gamma}{2\delta}\right)^2(1 - 2\delta^2), \quad (22)$$

expressed in terms of our fundamental parameters γ and δ . The current value of j_P in the last equation is positive (for small values of δ), but the Pioneer acceleration, as in (11) or (19), is considered negative in this paper so that a positive jerk means that the absolute value of a_P will decrease for increasing times or radial distances, which is indeed shown in the early Pioneer data, as it was already mentioned at the beginning of this section.

In Figure 2, we illustrate the early Pioneer 10/11 data, as originally reported in [30], where the absolute value of the Pioneer acceleration $|a_P|$ is plotted as a function of the radial heliocentric distance in AU. The red-dashed horizontal line and the green-dotted lines represent, respectively,

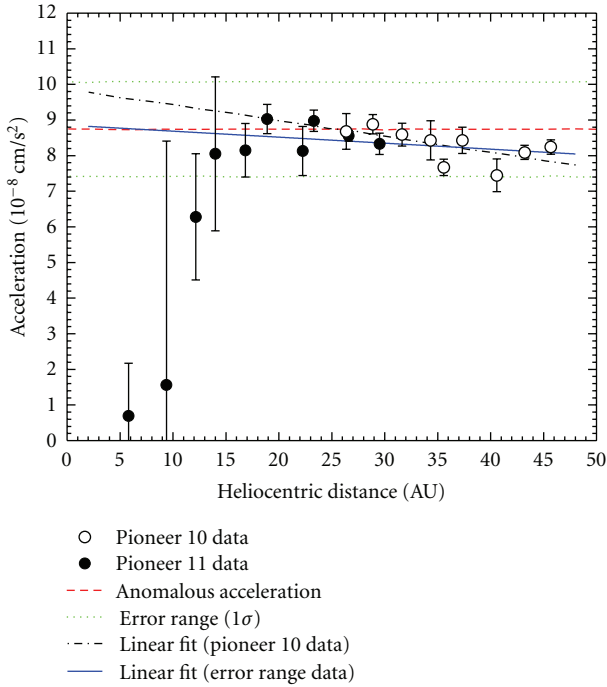


FIGURE 2: Early data for Pioneer 10/11 acceleration as a function of heliocentric distance. The average value of the anomalous acceleration is indicated in red-dashed, together with its error range (green-dotted). We also show linear fits of the data, which allow for the determination of our cosmological parameters γ and δ .

the value of $|a_p|$ and the related 1-sigma error range quoted in (11). The first three data points for Pioneer 11, at smaller distances, lie outside the considered error range probably because the anomalous acceleration was masked by solar radiation or other effects. We will not include these first three data points in our subsequent discussion. We will concentrate our analysis on either just the Pioneer 10 data points or the combination of data points for both spacecraft, but within the 1-sigma error range (“error range data” in the following).

These two sets of data clearly show a possible decrease of the Pioneer anomaly (in the absolute value $|a_p|$) with increasing heliocentric distance. The black (dash-dotted) line and the blue-solid line in the same figure represent linear fits for the Pioneer 10 and the error range data, respectively, both of them indicating a decrease of $|a_p|$.

If our conformal cosmology is the origin of the Pioneer anomaly, and not the thermal recoil force mentioned at the beginning of this section, our “jerk” equation (22) will explain the decrease of $|a_p|$ and can also be used to determine our second parameter δ .

We computed the slopes of our two linear fits in Figure 2 and used them as (positive) values of j_p in (22), together with the γ value from (20). (The radial distances r of the data plotted in Figure 2 were converted into elapsed times t' , by using a simple approximation: $r \simeq v_P t'$, where v_P is the average Pioneer speed. From the original data (available from the NASA website at: <http://cohoweb.gsfc.nasa.gov/helios/>),

we estimated $v_{P10} \simeq 12.96$ km/s, $v_{P11} \simeq 11.42$ km/s, and used an average $v_P \simeq 12.19$ km/s when combining data for both spacecraft.) Solving (22) for δ , we obtain

$$\begin{aligned} j_P &= (3.85 \pm 1.88) \times 10^{-17} \text{ cm s}^{-3} \quad (\text{Pioneer 10 data}), \\ \delta &= (8.12 \pm 2.35) \times 10^{-5}, \\ j_P &= (1.37 \pm 0.95) \times 10^{-17} \text{ cm s}^{-3} \quad (\text{error range data}), \\ \delta &= (1.36 \pm 0.52) \times 10^{-4}, \end{aligned} \quad (23)$$

and these values for δ are very close to the one we obtained in [29] ($\delta_0 = 3.83 \times 10^{-5}$), which was based solely on the analysis of type-Ia Supernovae data.

Another type of analysis is illustrated in Figure 3. The Pioneer 10/11 data, the standard value of $|a_p|$, and the related error range are the same as in the previous figure, but this time we used the generalized expression of a_p in (21) to fit the data within the error range. We allowed both quantities γ and δ to be free parameters in our fitting procedure, and we converted the elapsed time t' in (21) into the radial distance r by using the approximation $r \simeq v_P t'$, where v_P is the average Pioneer speed, as it was done also for the data in the previous figure. The radial distance r should be more properly identified with the geocentric distance of the spacecraft, rather than the heliocentric one, since r should be the distance from the Earth observer. We also performed fits using the geocentric distance, but the results were very similar to those obtained by using heliocentric distances, so we will not include them in the following analysis.

Again, in Figure 3, we used the expression in (21) to fit the data, although the fitting curves appear almost as straight lines in this figure. The first conformal cosmology fit, illustrated by the black (dash-dotted) curve, was obtained by using only the Pioneer 10 data and yielded the following values of the parameters:

$$\begin{aligned} \delta &= (9.19 \pm 1.53) \times 10^{-5} \quad (\text{Pioneer 10 data}), \\ \gamma &= (2.20 \pm 0.18) \times 10^{-28} \text{ cm}^{-1}. \end{aligned} \quad (24)$$

The second fit (blue-solid curve) was obtained by using all the data within the error range (again omitting the first three Pioneer 11 data points) and produced the following results:

$$\begin{aligned} \delta &= (1.38 \pm 0.43) \times 10^{-4} \quad (\text{error range data}), \\ \gamma &= (1.97 \pm 0.08) \times 10^{-28} \text{ cm}^{-1}. \end{aligned} \quad (25)$$

Comparing the results in the last two equations with those for δ in (23), obtained with a fixed $\gamma = 1.94 \times 10^{-28} \text{ cm}^{-1}$ as in (20), we can see that all the values of our parameters are in agreement. In particular, from the different analyses, we consistently obtain $\gamma \simeq 1.9\text{--}2.2 \times 10^{-28} \text{ cm}^{-1}$ and $\delta \sim 10^{-4}\text{--}10^{-5}$, where the different values depend on the Pioneer data being used. As already remarked, the values for δ quoted above are also close to the one we obtained in [29] ($\delta_0 = 3.83 \times 10^{-5}$), based on type-Ia Supernovae data. In the next section, we will discuss our results and compare

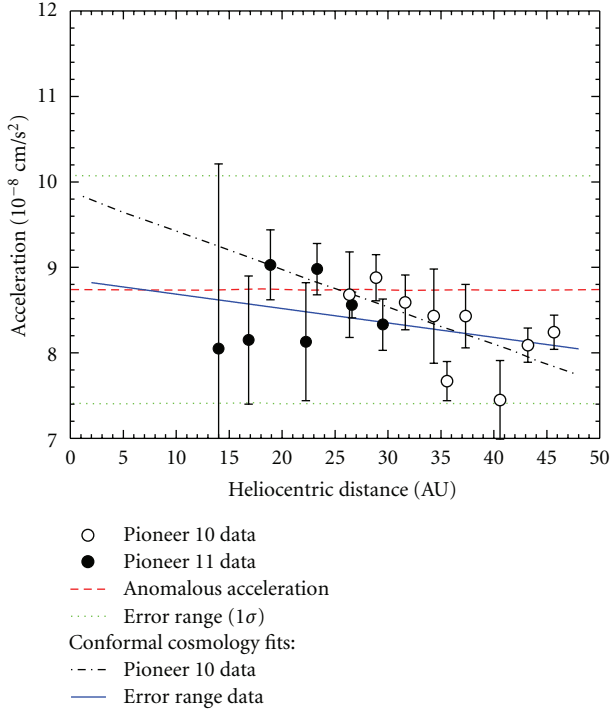


FIGURE 3: Early data for Pioneer 10/11 acceleration as a function of heliocentric distance. The average value of the anomalous acceleration is indicated in red-dashed, together with its error range (green-dotted). We also show full conformal cosmology fits of the data, which allow for a better determination of our cosmological parameters γ and δ .

them to the current limits of standard gravity in the solar system.

As already mentioned at the beginning of this paper, a new analysis of extended Pioneer data has recently appeared [31], and these new results will also be discussed in the next section. However, complete new data points from this extended analysis are not yet available but will be published in the future [31]. Due to this reason, we have based our analysis in this section only on the early Pioneer data which were available at the time of our study.

4. Discussion of Our Results and Conclusions

In the previous sections, we discussed how conformal cosmology provides a natural explanation for the Pioneer anomalous acceleration, in both magnitude and direction (i.e., the negative sign of the radial acceleration). We also explained the “numerical coincidence,” connecting a_P with the Hubble constant, and the observed decrease with heliocentric distance of $|a_P|$, related to the Pioneer jerk j_P . Although the Pioneer data are still not very accurate, our analysis consistently indicated that our conformal parameters are approximately given by $\gamma \sim 10^{-28} \text{ cm}^{-1}$ and $\delta \sim 10^{-4} - 10^{-5}$ (see (10), (20), and (23)–(25)). In this final section, we will discuss the implications of the values of our parameters in relation to other studies in the field.

We first remark that a new analysis of rotational velocity data for spiral galaxies, based on conformal gravity, has recently appeared ([59, 60]) improving the original work on the subject ([32, 33]). This new study uses the full line element of conformal gravity in (1)–(2), including the effects of the quadratic term $-\kappa r^2$, which were previously neglected, thus obtaining a global gravitational potential $V_{\text{global}}(r) = (\gamma/2)c^2 r - (\kappa/2)c^2 r^2$ of cosmological origin. In addition to this, a local gravitational potential $V_{\text{local}}(r)$ is obtained by integrating over the visible galactic mass distribution a gravitational potential per unit solar mass of the form $V^*(r) = -G(M_\odot/r) + (\gamma^*/2)c^2 r$. The two potentials, global and local, are then combined together to model the rotational motion of galaxies. The fits to galactic rotation data ([59, 60]), performed without any dark matter contribution, show a remarkable success of conformal gravity, even at the largest distances from the galactic centers, where the quadratic term $-\kappa r^2$ becomes important and comparable to the linear term γr . Mannheim and collaborators ([59, 60]) were then able to determine the values of the global universal parameters as $\gamma_{\text{Mann}} = 3.06 \times 10^{-30} \text{ cm}^{-1}$ and $\kappa_{\text{Mann}} = 9.54 \times 10^{-54} \text{ cm}^{-2}$. The related terms of the global gravitational potential were associated respectively to the cosmological background and to cosmological inhomogeneities. The local parameter γ^* was also evaluated as $\gamma^* = 5.42 \times 10^{-41} \text{ cm}^{-1}$.

The values of the dimensionful parameters γ and κ obtained through this analysis of galactic rotation curves are somewhat different from our values, reported in this paper or in our previous work [29] ($\gamma_0 = 1.94 \times 10^{-28} \text{ cm}^{-1}$ and $\kappa_0 = 6.42 \times 10^{-48} \text{ cm}^{-2}$). This difference could be due, as we explained in [29], to a possible redefinition of the luminosity distance and other distance indicators, which might affect even the radial distances (from the galactic centers) which are employed in the galactic rotation analysis.

However, it is instructive to compute the dimensionless δ parameter, using Mannheim’s values γ_{Mann} and κ_{Mann} , because this dimensionless constant should not be affected by a revision of the cosmological distances. As explained at the beginning of Section 2, the parameters k , γ , κ , and δ are related through $k = -\gamma^2/4 - \kappa$ and also $\delta = (\gamma/2\sqrt{|k|})$ so that we obtain

$$\begin{aligned} k_{\text{Mann}} &\simeq -\kappa_{\text{Mann}} = -9.54 \times 10^{-54} \text{ cm}^{-2}, \\ \delta_{\text{Mann}} &= 4.95 \times 10^{-4}. \end{aligned} \quad (26)$$

Therefore, the conformal gravity analysis by Mannheim and collaborators suggests a $\mathbf{k} \equiv k/|k| = -1$ Universe, consistent with our cosmological model and also a value of $\delta_{\text{Mann}} = 4.95 \times 10^{-4}$, close to our quoted values of $\delta \sim 10^{-4} - 10^{-5}$.

Conformal gravity considers local gravitational effects as being due to the local potential V_{local} or simply to the potential $V^*(r) = -G(M_\odot/r) + (\gamma^*/2)c^2 r$, where r is the radial distance from the center of our solar system. Since the value of the local constant $\gamma^* \sim 10^{-41} \text{ cm}^{-1}$ is very small, the modifications to standard dynamics of the solar system are negligible. (For example, the ratio between the conformal gravitational potential $(\gamma^*/2)c^2 r$ and the standard Newtonian term $G(M_\odot/r)$ at a heliocentric distance of 1 AU is $\sim 10^{-20}$, while, at a distance of 100 AU (outer solar system),

the same ratio is $\sim 10^{-16}$. The galactic potential, related to another conformal gravity term of the form $(\gamma_{\text{Mann}}/2)c^2 r'$ (r' distance from galactic center) would generate only a very small tidal force effect on the solar system. This correction would behave as the ratio of the distance of a planet or satellite from the sun divided by the distance from the solar system to the center of the galaxy [61]. Therefore, the “conformal gravity force” is negligible, compared to the standard Newtonian one, over the whole solar system region.) Therefore, conformal gravity is not in any way in contradiction with the very stringent limits on alternative gravity theories imposed by studies of planetary ephemerides or other solar system observations ([62, 63]).

In particular, more recent studies have focused their attention on the critical issue of the influence that a gravitational Pioneer anomaly acceleration would have on the motion of bodies in the solar system, such as inner and outer planets, comets, and asteroids ([64–75]). These studies indicate that an anomalous acceleration of gravitational origin would have a significant effect on the motion of these solar system objects, but the resulting orbital anomalies were not detected in the latest observations, therefore ruling out the gravitational origin of the Pioneer anomaly. As already mentioned above, we also believe that the dynamical corrections due to conformal gravity are in fact negligible at the solar system level. Therefore, no significant changes in the orbits of bodies in the solar system should be detected, in agreement with the cited references.

To further clarify the issue, in our analysis of the Pioneer anomaly, we used the reported values of the anomalous acceleration a_P to determine the cosmological parameters, simply because such was the way these data were reported in the literature cited. However, it should be clear from the discussion in Section 3 that we explain the Pioneer anomaly in terms of our *cosmological-gravitational blueshift*, based on the global values of the parameters γ , κ , and δ . In this view, there is no real dynamic acceleration of the Pioneer spacecraft (or of any other object in the solar system) oriented toward the Sun, due to some new gravitational force or modification of existing gravity, except for the tiny corrections coming from local conformal gravity mentioned above. In fact, in our analysis, we assume that there is no difference between the two velocities $v_{\text{mod}}(t')$ and $v_{\text{obs}}(t')$ in (13) and (15); therefore, the anomalous acceleration defined as $a_P \equiv d(\Delta v)/dt' \simeq [\Delta v(t' + \Delta t') - \Delta v(t')]/\Delta t'$ with $\Delta v = v_{\text{obs}} - v_{\text{mod}}$ is actually zero.

In this way, we also overcome the original objection, reported in [4], that “the anomalous acceleration is too large to have gone undetected in planetary orbits, particularly for Earth and Mars,” since “NASA’s Viking mission provided radio-ranging measurements [76] to an accuracy of about 12 m,” which should have shown the effect of the anomalous acceleration on the orbits of these two planets.

In our view, precision ranging measurements with radio signals or lasers, based on the round-trip travel time from Earth to other bodies in the solar system, would not show any anomalous effect because the speed of light is not affected by our cosmological model and the corrections to the dynamics of the solar system due to conformal gravity are negligible.

On the contrary, we would observe an effect similar to the anomalous acceleration for a spacecraft, a planet, or any other object in the solar system, if we were to study its motion through Doppler frequency ranging, because of the intrinsic differences in frequency or wavelength for light emitted at different spacetime positions, due to our cosmological model.

A similar discussion can be done regarding possible explanations of the Pioneer anomaly of cosmological origin. Recent studies based on the standard Friedmann-Lemaitre metric ([77, 78]) have shown that cosmological effects fail to account for the anomaly by several orders of magnitude. Again, our study does not propose dynamical corrections to the orbits, due to conformal gravity or to a conformal cosmological model, since these corrections would be negligible in the solar system, as are those due to standard cosmology. Our model simply assumes the existence of a local blueshift region, which is able to affect the frequencies of the signals exchanged between the spacecraft and Earth.

The size of the local blueshift region, which in our model is responsible for the frequency differences, can be easily estimated by using (9) and the values of our parameters. For example, using the values from our conformal cosmology fits in (24) and (25), we obtain $r_{\text{rs}} \simeq 50\text{--}126$ pc, corresponding to a distance comparable to the one between Earth and the nearest bright stars (which is about 15–30 pc). This blueshift region would extend well beyond the solar system but would cover a small portion of our galaxy, since $r_{\text{MilkyWay}} \simeq 14.6$ kpc.

The maximum blueshift effect would be seen at $r = (1/2)r_{\text{rs}} \simeq 25\text{--}63$ pc and would correspond to a $z_{\text{min}} = \sqrt{1 - \delta^2} - 1 \sim -10^{-8}$, a very small value. Therefore, the blueshift region and the related effects are so small that they cannot be practically observed in the radiation spectrum of stars or other radiation-emitting objects within this region. These effects are only small corrections to the Doppler signals coming from the Pioneer or other similar spacecraft.

We also want to compare our estimates of the rate of change of the anomalous acceleration (i.e., the jerk j_P) with those presented by independent verifications of the Pioneer anomaly (see review in [1]). The first of these studies was performed by Markwardt [58], who reviewed data for Pioneer 10 and reported $a_{P10} = -(7.70 \pm 0.02) \times 10^{-8}$ cm/s², with $j_{P10} < 0.18 \times 10^{-8}$ cm/s²/year = 5.70×10^{-17} cm/s³. (We prefer to report here, as also done in the rest of the paper, the anomalous acceleration a_P as a negative quantity and the related jerk j_P as a positive quantity. Some of the papers in the literature adopt the opposite sign convention, which might generate some confusion.) Using Markwardt values in (19) and (22), we obtain $\gamma_{\text{Mark}} = 1.71 \times 10^{-28}$ cm⁻¹ and $\delta_{\text{Mark}} = 5.89 \times 10^{-5}$, consistent with our values in (20) and (23)-(24) for Pioneer 10.

The second independent study was done by Toth [79] and reported results separately for the two spacecraft. From Toth’s results for Pioneer 10 ($a_{P10} = -(10.96 \pm 0.89) \times 10^{-8}$ cm/s², $j_{P10} = (0.21 \pm 0.04) \times 10^{-8}$ cm/s²/year = 6.65×10^{-17} cm/s³), we compute $\gamma_{\text{TothP10}} = 2.44 \times 10^{-28}$ cm⁻¹ and

$\delta_{\text{Toth}P10} = 7.76 \times 10^{-5}$. Using instead Toth's results for Pioneer 11 ($a_{P11} = -(9.40 \pm 1.12) \times 10^{-8} \text{ cm/s}^2$, $j_{P11} = (0.34 \pm 0.12) \times 10^{-8} \text{ cm/s}^2/\text{year} = 1.08 \times 10^{-16} \text{ cm/s}^3$), we obtain $\gamma_{\text{Toth}P11} = 2.09 \times 10^{-28} \text{ cm}^{-1}$ and $\delta_{\text{Toth}P11} = 5.23 \times 10^{-5}$, and all these results are also consistent with those discussed in Section 3.

Finally, we wish to comment briefly on the recent analysis of extended Pioneer data by Turyshev and collaborators [31]. This new study confirmed the anomalous acceleration and its temporal decrease in absolute value ($d|a_P|/dt \simeq -0.17 \times 10^{-8} \text{ cm/s}^2/\text{year} \simeq -5.4 \times 10^{-17} \text{ cm/s}^3$) using data spans more than twice as long as those used in previous studies. To analyze the temporal behavior, different models were used including a linear fit similar to the one which was employed in our analysis. Their results were reported separately for the two spacecrafts as follows (using our sign conventions).

Pioneer 10: $a_{P10} = -(11.06 \pm 0.08) \times 10^{-8} \text{ cm/s}^2$, $j_{P10} = (0.17 \pm 0.01) \times 10^{-8} \text{ cm/s}^2/\text{year} = 5.39 \times 10^{-17} \text{ cm/s}^3$, from which we compute $\gamma_{\text{Turyshv}P10} = 2.46 \times 10^{-28} \text{ cm}^{-1}$ and $\delta_{\text{Turyshv}P10} = 8.70 \times 10^{-5}$. Pioneer 11: $a_{P11} = -(11.65 \pm 0.42) \times 10^{-8} \text{ cm/s}^2$, $j_{P11} = (0.18 \pm 0.03) \times 10^{-8} \text{ cm/s}^2/\text{year} = 5.70 \times 10^{-17} \text{ cm/s}^3$, from which we obtain $\gamma_{\text{Turyshv}P11} = 2.59 \times 10^{-28} \text{ cm}^{-1}$ and $\delta_{\text{Turyshv}P11} = 8.90 \times 10^{-5}$. Therefore, these results are also in agreement with those discussed in Section 3. A more detailed comparison of the latest Pioneer results [31] with those obtained using conformal cosmology will be presented in a future study on the subject.

In conclusion, the detailed analysis of the Pioneer anomaly presented in this work has indicated that our conformal cosmology might be the origin of this effect, while conformal gravity alone cannot account for the anomalous acceleration of the spacecraft. If our analysis is correct, it explains naturally the numerical coincidence between the Pioneer acceleration and the Hubble constant, including the signs of these quantities. In addition, we confirm our previous evaluations of the cosmological parameters, $\gamma_0 = (1.94 \pm 0.30) \times 10^{-28} \text{ cm}^{-1}$ and $\delta_0 = 3.83 \times 10^{-5}$, also in agreement with independent evaluations. Further studies will be needed when the reanalysis of all the historical navigational data for the Pioneer spacecraft will be completed by Turyshev and collaborators, and new data will be publicly available.

Acknowledgments

This work was supported by a grant from the Frank R. Seaver College of Science and Engineering, Loyola Marymount University. The author would like to acknowledge Dr. S. Turyshev and Dr. P. Mannheim for very useful discussions and advice on the subject. The author also thanks the anonymous reviewers for the useful comments which helped improve the final version of the paper.

References

- [1] S. G. Turyshev and V. T. Toth, "The pioneer anomaly," *Living Reviews in Relativity*, vol. 13, no. 4, pp. 9–175, 2010.
- [2] J. D. Anderson, P. A. Laing, E. L. Lau, A. S. Liu, M. M. Nieto, and S. G. Turyshev, "Indication, from pioneer 10/11, Galileo, and Ulysses data, of an apparent anomalous, weak, long-range

- acceleration," *Physical Review Letters*, vol. 81, no. 14, pp. 2858–2861, 1998.
- [3] S. G. Turyshev, J. D. Anderson, P. A. Laing, E. L. Lau, A. S. Liu, and M. M. Nieto, "The apparent anomalous, weak, long-range acceleration of pioneer 10 and 11," <http://arxiv.org/abs/gr-qc/9903024>.
- [4] J. D. Anderson, P. A. Laing, E. L. Lau, A. S. Liu, M. M. Nieto, and S. G. Turyshev, "Study of the anomalous acceleration of Pioneer 10 and 11," *Physical Review D*, vol. 65, no. 8, Article ID 082004, pp. 820041–820045, 2002.
- [5] C. Lämmerzahl, O. Preuss, and H. Dittus, "Is the physics within the Solar system really understood?" in *Lasers, Clocks and Drag-Free Control: Exploration of Relativistic Gravity in Space*, H. Dittus, C. Lämmerzahl, and S. G. Turyshev, Eds., vol. 349 of *Astrophysics and Space Science Library*, p. 75, 2008.
- [6] J. D. Anderson and M. M. Nieto, "Astrometric solar-system anomalies," in *Relativity in Fundamental Astronomy: Dynamics, Reference Frames, and Data Analysis*, S. A. Klioner, P. K. Seidelmann, and M. H. Soffel, Eds., Proceedings IAU Symposium no. 261, pp. 189–197, 2010.
- [7] G. A. Krasinsky and V. A. Brumberg, "Secular increase of astronomical unit from analysis of the major planet motions, and its interpretation," *Celestial Mechanics and Dynamical Astronomy*, vol. 90, no. 3–4, pp. 267–288, 2004.
- [8] J. D. Anderson, J. K. Campbell, and M. M. Nieto, "The energy transfer process in planetary flybys," *New Astronomy*, vol. 12, no. 5, pp. 383–397, 2007.
- [9] J. D. Anderson, J. K. Campbell, J. E. Ekelund, J. Ellis, and J. F. Jordan, "Anomalous orbital-energy changes observed during spacecraft flybys of Earth," *Physical Review Letters*, vol. 100, no. 9, Article ID 091102, 2008.
- [10] S. G. Turyshev and V. T. Toth, "The puzzle of the flyby anomaly," *Space Science Reviews*, vol. 148, no. 1–4, pp. 169–174, 2009.
- [11] L. Iorio, "The recently determined anomalous perihelion precession of saturn," *Astronomical Journal*, vol. 137, no. 3, pp. 3615–3618, 2009.
- [12] L. Iorio, "The perihelion precession of Saturn, planet X/Nemesis and MOND," *The Open Astronomy Journal*, vol. 3, no. 1, 14 pages, 2010.
- [13] L. Iorio, "On the anomalous secular increase of the eccentricity of the orbit of the Moon," *Monthly Notices of the Royal Astronomical Society*, vol. 415, no. 2, pp. 1266–1275, 2011.
- [14] L. Iorio, "An empirical explanation of the anomalous increases in the astronomical unit and the lunar eccentricity," *Astronomical Journal*, vol. 142, no. 3, article 68, 2011.
- [15] E. V. Pitjeva, "EPM ephemerides and relativity," in *Relativity in Fundamental Astronomy: Dynamics, Reference Frames, and Data Analysis*, S. A. Klioner, P. K. Seidelmann, and M. H. Soffel, Eds., Proceedings IAU Symposium no. 261, pp. 170–178, Cambridge University Press, Cambridge, UK, 2010.
- [16] E. V. Pitjeva and N. P. Pitjev, "Estimations of changes of the Sun's mass and the gravitation constant from the modern observations of planets and spacecraft," <http://arxiv.org/abs/1108.0246>.
- [17] D. Grumiller, "Model for gravity at large distances," *Physical Review Letters*, vol. 105, no. 21, Article ID 211303, 2010.
- [18] S. Carloni, D. Grumiller, and F. Preis, "Solar system constraints on Rindler acceleration," *Physical Review D*, vol. 83, no. 12, Article ID 124024, 2011.
- [19] D. Grumiller and F. Preis, "Rindler force at large distances," <http://arxiv.org/abs/1107.2373>.
- [20] L. Iorio, "Solar system constraints on a Rindler-type extra-acceleration from modified gravity at large distances," *Journal*

- of Cosmology and Astroparticle Physics*, vol. 2011, no. 5, article 019, 2011.
- [21] L. Iorio, "Impact of a Pioneer/Rindler-type acceleration on the Oort cloud," <http://arxiv.org/abs/1108.0409>.
- [22] H. Weyl, "Reine Infinitesimalgeometrie," *Mathematische Zeitschrift*, vol. 2, pp. 384–411, 1918.
- [23] H. Weyl, "Gravitation und Elektrizität," *Sitzungsberichte der Preussischen Akademie der Wissenschaften. Physikalisch-Mathematische Klasse*, vol. 1, pp. 465–480, 1918.
- [24] H. Weyl, "Eine Neue Erweiterung der Relativitätstheorie," *Annalen der Physik*, vol. 59, pp. 101–103, 1919.
- [25] P. D. Mannheim and D. Kazanas, "Exact vacuum solution to conformal Weyl gravity and galactic rotation curves," *Astrophysical Journal*, vol. 342, p. 635, 1989.
- [26] D. Kazanas and P. D. Mannheim, "General structure of the gravitational equations of motion in conformal weyl gravity," *Astrophysical Journal, Supplement Series*, vol. 76, no. 2, pp. 431–453, 1991.
- [27] P. D. Mannheim, "Alternatives to dark matter and dark energy," *Progress in Particle and Nuclear Physics*, vol. 56, no. 2, pp. 340–445, 2006.
- [28] G. U. Varieschi, "A kinematical approach to conformal cosmology," *General Relativity and Gravitation*, vol. 42, no. 4, pp. 929–974, 2010.
- [29] G. U. Varieschi, "Kinematical conformal cosmology: fundamental parameters from astrophysical observations," *ISRN Astronomy and Astrophysics*, vol. 2011, Article ID 806549, 24 pages, 2011.
- [30] M. M. Nieto and J. D. Anderson, "Using early data to illuminate the Pioneer anomaly," *Classical and Quantum Gravity*, vol. 22, no. 24, pp. 5343–5354, 2005.
- [31] S. G. Turyshev, V. T. Toth, J. Ellis, and C. B. Markwardt, "Support for temporally varying behavior of the Pioneer anomaly from the extended Pioneer 10 and 11 doppler data sets," *Physical Review Letters*, vol. 107, no. 8, Article ID 081103, 2011.
- [32] P. D. Mannheim, "Linear potentials and galactic rotation curves," *Astrophysical Journal*, vol. 419, no. 1, pp. 150–154, 1993.
- [33] P. D. Mannheim, "Are galactic rotation curves really flat?" *Astrophysical Journal*, vol. 479, no. 2, pp. 659–664, 1997.
- [34] K. Nakamura and Particle Data Group, "Review of particle physics," *Journal of Physics A*, vol. G37, Article ID 075021, 2010.
- [35] J. D. Anderson, E. L. Lau, S. G. Turyshev, P. A. Laing, and M. M. Nieto, "Search for a standard explanation of the pioneer anomaly," *Modern Physics Letters A*, vol. 17, no. 14, pp. 875–885, 2002.
- [36] S. G. Turyshev, M. M. Nieto, and J. D. Anderson, "Study of the Pioneer anomaly: a problem set," *American Journal of Physics*, vol. 73, no. 11, pp. 1033–1044, 2005.
- [37] S. G. Turyshev, V. T. Toth, L. R. Kellogg, E. L. Lau, and K. J. Lee, "A study of the pioneer anomaly: new data and objectives for new investigation," *International Journal of Modern Physics D*, vol. 15, no. 1, pp. 1–55, 2006.
- [38] V. T. Toth and S. G. Turyshev, "The Pioneer anomaly: seeking an explanation in newly recovered data," *Canadian Journal of Physics*, vol. 84, no. 12, pp. 1063–1087, 2006.
- [39] V. T. Toth and S. G. Turyshev, "Pioneer anomaly: evaluating newly recovered data," in *Proceedings of the 3rd Mexican Meeting on Mathematical and Experimental Physics*, vol. 977 of *AIP Conference Proceedings*, pp. 264–283, September 2007.
- [40] M. M. Nieto and J. D. Anderson, "Search for a solution of the Pioneer anomaly," *Contemporary Physics*, vol. 48, no. 1, pp. 41–54, 2007.
- [41] V. T. Toth and S. G. Turyshev, "Thermal recoil force, telemetry, and the Pioneer anomaly," *Physical Review D*, vol. 79, no. 4, Article ID 043011, 2009.
- [42] S. G. Turyshev and V. T. Toth, "The pioneer anomaly in the light of new data," *Space Science Reviews*, vol. 148, no. 1–4, pp. 149–167, 2009.
- [43] S. G. Turyshev and V. T. Toth, "Physics engineering in the study of the pioneer anomaly," <http://arxiv.org/abs/0710.0191>.
- [44] S. Turyshev, private communication, 2010.
- [45] J. D. Anderson, M. M. Nieto, and S. G. Turyshev, "A mission to test the Pioneer anomaly," *International Journal of Modern Physics D*, vol. 11, no. 10, pp. 1545–1551, 2002.
- [46] M. M. Nieto, S. G. Turyshev, and J. D. Anderson, "The pioneer anomaly: the data, its meaning, and a future test," in *Proceedings of the 2nd Mexican Meeting on Mathematical and Experimental Physics*, vol. 758 of *AIP Conference Proceedings*, pp. 113–128, September 2004.
- [47] H. Dittus, S. G. Turyshev, C. Lämmerzahl et al., "A mission to explore the Pioneer anomaly," in *Proceedings of the 39th ESLAB Symposium: Trends in Space Science and Cosmic Vision 2020*, ESA Spec.Publ. 588, pp. 3–10, April 2005.
- [48] S. G. Turyshev, M. M. Nieto, and J. D. Anderson, "A route to understanding of the pioneer anomaly," in *Proceedings of the 22nd Texas Symposium on Relativistic Astrophysics*, December 2004, paper no. 0310.
- [49] M. M. Nieto and S. G. Turyshev, "Finding the origin of the Pioneer anomaly," *Classical and Quantum Gravity*, vol. 21, no. 17, pp. 4005–4023, 2004.
- [50] O. Bertolami, F. Francisco, P. J. S. Gil, and J. Páramos, "Thermal analysis of the Pioneer anomaly: a method to estimate radiative momentum transfer," *Physical Review D*, vol. 78, no. 10, Article ID 103001, 2008.
- [51] B. Rievers, C. Lämmerzahl, M. List, S. Bremer, and H. Dittus, "New powerful thermal modelling for high-precision gravity missions with application to Pioneer 10/11," *New Journal of Physics*, vol. 11, Article ID 113032, 2009.
- [52] O. Bertolami, F. Francisco, P. J. S. Gil, and J. Páramos, "Estimating radiative momentum transfer through a thermal analysis of the pioneer anomaly," *Space Science Reviews*, vol. 151, no. 1–3, pp. 75–91, 2010.
- [53] B. Rievers, S. Bremer, M. List, C. Lämmerzahl, and H. Dittus, "Thermal dissipation force modeling with preliminary results for Pioneer 10/11," *Acta Astronautica*, vol. 66, no. 3–4, pp. 467–476, 2010.
- [54] B. Rievers, C. Lämmerzahl, and H. Dittus, "Modeling of thermal perturbations using raytracing method with preliminary results for a test case model of the pioneer 10/11 radioisotopic thermal generators," *Space Science Reviews*, vol. 151, no. 1–3, pp. 123–133, 2010.
- [55] B. Rievers and C. Lämmerzahl, "High precision thermal modeling of complex systems with application to the flyby and Pioneer anomaly," *Annalen der Physik (Leipzig)*, vol. 523, no. 6, pp. 439–449, 2011.
- [56] F. Francisco, O. Bertolami, P. J. S. Gil, and J. Páramos, "Modelling the reflective thermal contribution to the acceleration of the Pioneer spacecraft," <http://arxiv.org/abs/1103.5222>.
- [57] S. Weinberg, *Gravitation and Cosmology: Principles and Applications of the General Theory of Relativity*, John Wiley & Sons, New York, NY, USA, 1972.
- [58] C. B. Markwardt, "Independent confirmation of the pioneer 10 anomalous acceleration," <http://arxiv.org/abs/gr-qc/0208046>.

- [59] P. D. Mannheim and J. G. O'Brien, "Impact of a global quadratic potential on galactic rotation curves," *Physical Review Letters*, vol. 106, no. 12, Article ID 121101, 2011.
- [60] P. D. Mannheim and J. G. O'Brien, "Fitting galactic rotation curves with conformal gravity and a global quadratic potential," <http://arxiv.org/abs/1011.3495>.
- [61] P. Mannheim, private communication, 2011.
- [62] E. M. Standish, "Planetary and Lunar Ephemerides: testing alternate gravitational theories," in *Recent Developments in Gravitation and Cosmology*, A. Macias, C. Lämmerzahl, and A. Camacho, Eds., vol. 977 of *AIP Conference Proceedings*, pp. 254–263, American Institute of Physics, Melville, NJ, USA, 2008.
- [63] E. M. Standish, "Testing alternate gravitational theories," in *Fundamental Astronomy: Dynamics, Reference Frames, and Data Analysis, Proceedings of the International Astronomical Union*, S. A. Klioner, P. K. Seidelmann, and M. H. Soffel, Eds., vol. 261 of *IAU Symposium*, pp. 179–182, 2010.
- [64] L. Iorio and G. Giudice, "What do the orbital motions of the outer planets of the Solar System tell us about the Pioneer anomaly?" *New Astronomy*, vol. 11, no. 8, pp. 600–607, 2006.
- [65] G. L. Page, D. S. Dixon, and J. F. Wallin, "Can minor planets be used to assess gravity in the outer solar system?" *Astrophysical Journal*, vol. 642, no. 1, pp. 606–614, 2006.
- [66] K. Tangen, "Could the Pioneer anomaly have a gravitational origin?" *Physical Review D*, vol. 76, no. 4, 2007.
- [67] L. Iorio, "Can the pioneer anomaly be of gravitational origin? A phenomenological answer," *Foundations of Physics*, vol. 37, no. 6, pp. 897–918, 2007.
- [68] L. Iorio, "Jupiter, Saturn and the Pioneer anomaly: a planetary-based independent test," *Journal of Gravitational Physics*, vol. 1, no. 1, pp. 5–8, 2007.
- [69] J. F. Wallin, D. S. Dixon, and G. L. Page, "Testing gravity in the outer solar system: results from trans-neptunian objects," *Astrophysical Journal*, vol. 666, no. 2, pp. 1296–1302, 2007.
- [70] L. Iorio, "The Lense-Thirring effect and the Pioneer anomaly: solar system tests," in *Proceedings of the the 11th Marcel Grossmann Meeting on Recent Developments in Theoretical and Experimental General Relativity, Gravitation and Relativistic Field Theorie*, H. Kleinert, R.T. Jantzen, and R. Ruffini, Eds., pp. 2558–2560, World Scientific, 2008.
- [71] A. Fienga, J. Laskar, P. Kuchynka, C. Leponcin-Lafitte, H. Manche, and M. Gastineau, "Gravity tests with INPOP planetary ephemerides," in *Relativity in Fundamental Astronomy*, S. A. Klioner, P. K. Seidelmann, and M. H. Soffel, Eds., Proceedings IAU Symposium no. 261, pp. 159–169, 2010.
- [72] G. L. Page, J. F. Wallin, and D. S. Dixon, "How well do we know the orbits of the outer planets?" *Astrophysical Journal*, vol. 697, no. 2, pp. 1226–1241, 2009.
- [73] L. Iorio, "Does the Neptunian system of satellites challenge a gravitational origin for the Pioneer anomaly," *Monthly Notices of the Royal Astronomical Society*, vol. 405, no. 4, pp. 2615–2622, 2010.
- [74] G. L. Page, "Exploring the weak limit of gravity at solar system scales," *Publications of the Astronomical Society of the Pacific*, vol. 122, no. 888, pp. 259–260, 2010.
- [75] L. Iorio, "Orbital effects of the time-dependent component of the Pioneer anomaly," <http://arxiv.org/abs/1107.3445>.
- [76] R.D. Reasenberg, I. I. Shapiro, P. E. MacNeil et al., "Viking relativity experiment: verification of signal retardation by solar gravity," *Astrophysical Journal*, vol. 234, pp. L219–L221, 1979.
- [77] M. Mizony and M. Lachièze-Rey, "Cosmological effects in the local static frame," *Astronomy and Astrophysics*, vol. 434, no. 1, pp. 45–52, 2005.
- [78] M. Lachièze-Rey, "Cosmology in the solar system: the Pioneer effect is not cosmological," *Classical and Quantum Gravity*, vol. 24, no. 10, article 016, pp. 2735–2742, 2007.
- [79] V. T. Toth, "Independent analysis of the orbits of pioneer 10 and 11," *International Journal of Modern Physics D*, vol. 18, no. 5, pp. 717–741, 2009.